⌘ *Author's Choice*

THE JOURNAL OF BIOLOGICAL CHEMISTRY VOL. 285, NO. 45, pp. 34355–34363, November 5, 2010

New Hierarchical Phosphorylation Pathway of the Translational Repressor eIF4E-binding Protein 1 (4E-BP1) in Ischemia-Reperfusion Stress*[S]

Received for publication, April 19, 2010, and in revised form, August 22, 2010 Published, JBC Papers in Press, August 24, 2010, DOI 10.1074/jbc.M110.135103

María I. Ayuso, Macarena Hernández-Jiménez, María E. Martín[1], Matilde Salinas, and Alberto Alcázar[2]

From the Department of Investigation, Hospital Ramón y Cajal, 28034 Madrid, Spain

Eukaryotic initiation factor (eIF) 4E-binding protein 1 (4E-BP1) is a translational repressor that is characterized by its capacity to bind specifically to eIF4E and inhibit its interaction with eIF4G. Phosphorylation of 4E-BP1 regulates eIF4E availability, and therefore, cap-dependent translation, in cell stress. This study reports a physiological study of 4E-BP1 regulation by phosphorylation using control conditions and a stress-induced translational repression condition, ischemia-reperfusion (IR) stress, in brain tissue. In control conditions, 4E-BP1 was found in four phosphorylation states that were detected by two-dimensional gel electrophoresis and Western blotting, which corresponded to Thr^{69}-phosphorylated alone, Thr^{69}- and Thr^{36}/Thr^{45}-phosphorylated, all these plus Ser^{64} phosphorylation, and dephosphorylation of the sites analyzed. In control or IR conditions, no Thr^{36}/Thr^{45} phosphorylation alone was detected without Thr^{69} phosphorylation, and neither was Ser^{64} phosphorylation without Thr^{36}/Thr^{45}/Thr^{69} phosphorylation detected. Ischemic stress induced 4E-BP1 dephosphorylation at Thr^{69}, Thr^{36}/Thr^{45}, and Ser^{64} residues, with 4E-BP1 remaining phosphorylated at Thr^{69} alone or dephosphorylated. In the subsequent reperfusion, 4E-BP1 phosphorylation was induced at Thr^{36}/Thr^{45} and Ser^{64}, in addition to Thr^{69}. Changes in 4E-BP1 phosphorylation after IR were according to those found for Akt and mammalian target of rapamycin (mTOR) kinases. These results demonstrate a new hierarchical phosphorylation for 4E-BP1 regulation in which Thr^{69} is phosphorylated first followed by Thr^{36}/Thr^{45} phosphorylation, and Ser^{64} is phosphorylated last. Thr^{69} phosphorylation alone allows binding to eIF4E, and subsequent Thr^{36}/Thr^{45} phosphorylation was sufficient to dissociate 4E-BP1 from eIF4E, which led to eIF4E-4G interaction. These data help to elucidate the physiological role of 4E-BP1 phosphorylation in controlling protein synthesis.

An important control point in the translation process in eukaryotic organisms is the recruitment of the 40 S ribosomal subunit to the 5′ end of mRNA. A key step in this process is the assembly of eukaryotic initiation factor (eIF) 4F complex, which contains: the initiation factor eIF4A, an ATP-dependent RNA helicase; eIF4E, which binds to the mRNA 5′ cap structure m^7GpppN (7-methylguanosine triphosphate and N is any nucleotide); and eIF4G, a scaffolding protein that provides docking sites for the aforementioned initiation factors and binds the poly(A)-binding protein (PABP), thereby circularizing the mRNA (1–3). eIF4E recruits eIF4G and eIF4A to assemble the eIF4F complex and binds to the 5′ cap (3). The availability of eIF4E is a limiting step in translation initiation; therefore, eIF4E activity is a primary key for control of gene expression. The family of translational repressors named eIF4E-binding proteins (4E-BPs),[3] which in mammals comprise three members (4E-BP1, 4E-BP2, and 4E-BP3), shares with eIF4G a common binding motif to eIF4E that is mutually exclusive (2, 4). The activity of 4E-BPs is regulated through their phosphorylation. Active hypophosphorylated forms of 4E-BPs bind to eIF4E, compete with eIF4G, and inhibit eIF4G binding to eIF4E, which prevents eIF4F complex formation and inhibits cap-dependent translation (1–8). Conversely, (hyper)phosphorylation of 4E-BPs reduces their affinity for eIF4E and releases them from eIF4E. This allows eIF4E to bind eIF4G and formation of the eIF4F complex, which leads to translation activation (1–8).

In the best characterized 4E-BP protein, 4E-BP1 (also known as PHAS-I), seven different sites of phosphorylation have been mapped that correspond in the rodent 4E-BP1 sequence to Thr^{36}, Thr^{45}, Ser^{64}, Thr^{69}, Ser^{82}, Ser^{100}, and Ser^{111} (+1 in the human sequence). Four of these are known to be regulated via signaling pathways (Thr^{36}, Thr^{45}, Ser^{64}, and Thr^{69}), and these sites are conserved in 4E-BP1 proteins from different species, as well as in the two other 4E-BPs (6, 7). Phosphorylation of the other three sites appears not to be regulated (6, 9). 4E-BP1 is one of the main effectors of mammalian target of rapamycin (mTOR), serine/threonine-protein kinase in the phosphoinositide 3-kinase (PI3-kinase)/Akt (RAC serine/threonine-protein kinase, also named protein kinase B, PKB) signaling pathway that integrates signals from extracellular stimuli, amino acid availability, and oxygen and energy status of the cells (8). 4E-BPs contain a TOR signaling (TOS) motif that binds the mTOR complex 1 (mTORC1) (6). mTORC1 controls the activity of 4E-BP1. Activation of mTORC1 results in phosphoryla-

* This work was supported by Institute of Health Carlos III (ISCIII) Grants FIS08/0761 and RETICS-RD06/0026/008 from the Spanish Ministry of Science and Innovation, including a predoctoral position for M. I. A.

⌘ *Author's Choice*—Final version full access.

[S] The on-line version of this article (available at http://www.jbc.org) contains supplemental Figs. S1–S8.

[1] A researcher from Fundacion de Investigacion Biomedica del Hospital Universitario Ramón y Cajal (FIBio-HRC) supported by the Regional Government of Madrid.

[2] To whom correspondence should be addressed: Depto. Investigación, Hospital Ramón y Cajal, Ctra. Colmenar km 9.1, 28034 Madrid, Spain. Fax: 34-91-336-9016; E-mail: alberto.alcazar@hrc.es.

[3] The abbreviations used are: 4E-BP, eIF4E-binding protein; IR, ischemia-reperfusion; SHC, sham control; mTOR, mammalian target of rapamycin; mTORC1, mTOR complex 1; TOS, TOR signaling; ROS, reactive oxygen species; PMS, postmitochondrial supernatant; PP2A, protein phosphatase 2A.

tion of 4E-BP1 at Thr^{36}, Thr^{45}, Ser^{64}, and Thr^{69} sites and the release of 4E-BP1 from eIF4E (6, 7). These phosphorylation modifications follow a hierarchy; phosphorylation of Thr^{36}/Thr^{45} appears to be required as a priming event for subsequent phosphorylation of Thr^{69}, and Ser^{64} is phosphorylated last (10). However, their individual contribution to the control of eIF4E binding is controversial (6). Phosphorylation of Thr^{36}/Thr^{45} does not regulate the binding of 4E-BP1 to eIF4E directly (6), whereas phosphorylation at Ser^{64} and Thr^{69} is insufficient to prevent binding to eIF4E (10). The hierarchical phosphorylation of 4E-BP1 at these sites is stimulated by agents such as insulin, growth factors and serum, and in many cell types, this effect requires the presence of amino acids in the culture medium. This compelling evidence has been reported in stimulated cultured cells, including cell lines and transfected cells, and the physiological roles of these phosphorylation reactions in the normal control of 4E-BP1 remain to be fully established (6).

mTORC1 acts as cellular energy and oxygen availability sensor (8, 11). Energy depletion severely decreases mTORC1 activity (7, 11), and because the translation is a major consumer of cellular energy, mTORC1 inactivation through 4E-BP1 hypophosphorylation induces translation inhibition. In addition to cellular energy levels, the sufficiency of oxygen is also essential for cellular metabolism. Hypoxic stress results in mTORC1 inhibition (11). Hypoxic stress causes energy deprivation, and inhibition of mTORC1 by means of 4E-BP1 hypophosphorylation inhibits energy-consuming processes such as protein synthesis. Ischemia induces a transient period of hypoxia that induces failure of energy metabolism that is restored in the subsequent reperfusion period (12). Moreover, the initial period of reperfusion increases reactive oxygen species (ROS) production and induces additional stress (13). The stress that results from ischemia and ischemia-reperfusion (IR) affects different tissues. However, the brain, because of its high metabolic rate, limited energy stores, and critical dependence on aerobic metabolism, is known to be particularly sensitive to these stresses (13, 14). In addition, a second stress can be induced by long term reperfusion, although only selective brain regions (*e.g.* the hippocampal region CA1) are affected (15).

Previously, we have reported dephosphorylation of 4E-BP1 after ischemia and induction of 4E-BP1 phosphorylation during short term reperfusion (16). In this study, we investigated ischemic and IR stress to establish the physiological status of critical phosphorylation sites in 4E-BP1, at Thr^{36}/Thr^{45}, Ser^{64}, and Thr^{69}. In addition, 4E-BP1 phosphorylation sites were investigated after short and long term reperfusion in the cerebral cortex and hippocampal region CA1. We discovered a new hierarchical phosphorylation pathway for 4E-BP1 and suggest a new physiological outcome for the phosphorylation sites in 4E-BP1.

EXPERIMENTAL PROCEDURES

Materials—Rabbit polyclonal anti-4E-BP1, anti-phospho-4E-BP1 (Thr^{37} and/or Thr^{46}), anti-phospho-4E-BP1 (Ser^{65}), anti-phospho-4E-BP1 (Thr^{70}), and monoclonal anti-phospho-4E-BP1 (Ser^{65} 174A9) antibodies (all according to human sequences) were from Cell Signaling. Mouse monoclonal anti-eIF4E antibody was from BD Transduction Laboratories. Goat polyclonal anti-eIF4G antibody was from Santa Cruz Biotechnology. Rabbit polyclonal anti-mTOR and anti-phospho-mTOR (Ser^{2448}) antibodies were from Millipore and Cell Signaling, respectively. Rabbit polyclonal anti-Akt and monoclonal anti-phospho-Akt (Ser^{473}) and mouse monoclonal anti-phospho-Akt (Thr^{308}) antibodies were also from Cell Signaling. Mouse monoclonal anti-β-actin antibody was from Sigma. The chemicals used in isoelectric focusing and SDS-PAGE were purchased from Bio-Rad and GE Healthcare. All general chemicals were purchased from Sigma unless stated otherwise.

Animal Models of Ischemia and IR—Incomplete forebrain ischemia was induced in adult Wistar rats (mean body weight 300 g) by the previously described standard four-vessel occlusion model previously described in Refs. 16–18. On day 1, both vertebral arteries were irreversibly occluded after anesthesia. On day 2, both common carotid arteries were occluded for 15 min by small atraumatic clips to induce ischemia, and then the animals were sacrificed (I15 group). For IR, animals underwent 15 min of ischemia, and both clips were removed from the carotid arteries for reperfusion for 30 min or 3 days (R30 and R3d, respectively), and then the animals were sacrificed. Sham control (SHC and SHC3d) animals were prepared in the same way as for the R30 and R3d animals, respectively, without carotid occlusion. In all experiments, the cerebral cortex and hippocampal region CA1 were carefully dissected under a magnifying glass. All procedures associated with animal experiments were approved by the Ethics Committee of the Hospital Ramon y Cajal, Madrid, Spain.

Sample Preparation—Cerebral cortex and hippocampal CA1 regions from control and ischemic animals and those that underwent different reperfusion times were rapidly dissected. The samples were homogenized 1:5 (w/v) with buffer A (20 mM Tris-HCl, pH 7.5; 140 mM potassium chloride; 5 mM magnesium acetate; 1 mM dithiothreitol; 2 mM benzamidine; 1 mM EDTA; 2 mM EGTA; 10 μg/ml pepstatin A, leupeptin, and antipain; 20 mM sodium β-glycerophosphate; 20 mM sodium molybdate; 0.2 mM sodium orthovanadate), as described previously (16, 18). The homogenate was centrifuged at 11,000 $\times$ *g* for 15 min to obtain a postmitochondrial supernatant (PMS). All procedures were performed at 4 °C. The PMS fraction that corresponded to each animal was kept separately at −80 °C until used, and protein concentrations were determined.

Association of eIF4E with eIF4G and 4E-BP1—To study eIF4F complex formation and 4E-BP1 and eIF4G association with eIF4E, a cap-containing matrix was used as described previously (16, 19). PMS samples (300 μg) for each experimental condition were added to 7-methyl-GTP (m^7GTP)-Sepharose 4B (GE Healthcare) (30 μl of 50/50 slurry) and incubated for 30 min at 4 °C in buffer A that contained 100 mM potassium chloride and 100 μM GTP (200 μl). The beads were centrifuged at 2500 $\times$ *g* for 5 min and washed in the same buffer three times. The proteins were removed from m^7GTP-Sepharose with SDS loading buffer and subjected to SDS-PAGE or two-dimensional electrophoresis and Western blotting. The immunoblots were developed separately with the antibodies described above against eIF4G, eIF4E, and 4E-BP1 and quantified as described below.

Western Blotting—Samples of PMS (35 μg) or m^{7}GTP-Sepharose of each different experimental condition were analyzed by SDS-PAGE (7.5 and 15% acrylamide for eIF4G and eIF4E or 4E-BP1, respectively; 3% cross-linking). Gels from SDS-PAGE or from two-dimensional gel electrophoresis were transferred onto PVDF membranes (GE Healthcare). The membranes were incubated for 1 h at room temperature or overnight at 4 °C with the antibody against the specific protein to be detected, washed, incubated for 1 h with peroxidase-conjugated anti-mouse or anti-rabbit IgG (both from GE Healthcare) or peroxidase-conjugated anti-goat IgG (Santa Cruz Biotechnology), and developed with ECL reagent (GE Healthcare). Phospho-4E-BP1 and 4E-BP1 were analyzed in twin separate experiments to avoid cross-reaction between the different antibodies. For mTOR and Akt detection, the blots were probed with the phospho-specific antibody, stripped, and reprobed with the corresponding anti-protein antibody.

Two-dimensional Gel Electrophoresis—Samples of PMS (75 μg) or m^{7}GTP-Sepharose of each experimental condition were added to 8.5 M urea, 5% β-mercaptoethanol and loaded into horizontal isoelectric focusing slab gels as the first dimension. Isoelectric focusing was performed with immobilized pH 3–10 nonlinear gradient strips (10 cm) in a flatbed Multiphor II electrophoresis system (GE Healthcare), according to the manufacturer's instructions. The first dimension was combined with standard vertical slab SDS-PAGE in a second dimension for gel electrophoresis, as described previously (20, 21). SDS-PAGE was performed in 12% acrylamide (2.6% cross-linking) gels (1.0 mm thick), with an isoelectric focusing strip used as a stacking gel.

Statistical Analysis—Four to six different animals for each experimental condition or group were independently analyzed in duplicate, and their average values were considered for statistical analysis. The specific reaction in Western blotting was quantified with the ImageQuant TL software (GE Healthcare). Internal standards (actin) were included to normalize the different immunoblots. Data of the phospho-forms or phosphoproteins were expressed in arbitrary units with respect to the levels of total protein. The results (ratios) were expressed as mean ± S.E. of the 4–6 independent experiments run in duplicate. Each experiment was performed with a different animal. Statistical analysis was done by analysis of variance following Dunnett's post test, when analysis of variance was significant, to compare the data between the SHC, I15, and R30 experimental groups or by Student's *t* test to compare the data from the I15, R30, or R3d groups, with respect to the SHC3d control group, for each cerebral cortex or hippocampal CA1 region separately. Comparisons between the cerebral cortex and hippocampal CA1 region were done by paired *t* test. Statistical significance was set at $p < 0.05$ using Prism statistical software (GraphPad Software).

RESULTS

Ischemic Stress Induces Hypophosphorylated 4E-BP1 and IR Stress Induces Hyperphosphorylated 4E-BP1 at Thr^{36}/Thr^{45}, Ser^{64}, and Thr^{69} sites—4E-BP1 can be resolved in one-dimensional SDS-PAGE in three bands, which have been named as the α, β, and γ forms in order of decreasing electrophoretic mobility (19, 22). Thus, the γ form is designated as hyperphosphorylated 4E-BP1, with a slower mobility than the phosphorylated 4E-BP1, which is named as the β form, and this is slower than the un- or hypophosphorylated 4E-BP1 form designated as α (19, 22). We analyzed these phospho-forms of 4E-BP1 in ischemia and IR stress by SDS-PAGE and Western blotting. Ischemia (I15) induced a significant increase in the α form of 4E-BP1, in parallel with a decrease in the γ form. IR with short term reperfusion (R30) significantly induced the γ form when compared with the SHC control situation, in which the β form was the more abundant (Fig. 1, *4E-BP1*; supplemental Fig. S1). IR with long term reperfusion (R3d) did not induce any significant effect on 4E-BP1 phospho-forms in comparison with the SHC3d control (Fig. 1, *4E-BP1*). Except for I15, no significant changes in the β form were found among the different experimental conditions when compared with the controls. Also, there were no changes between the cerebral cortex and hippocampal CA1 region. The data for the quantification of the α, β, and γ forms of 4E-BP1 are shown in supplemental Fig. S1.

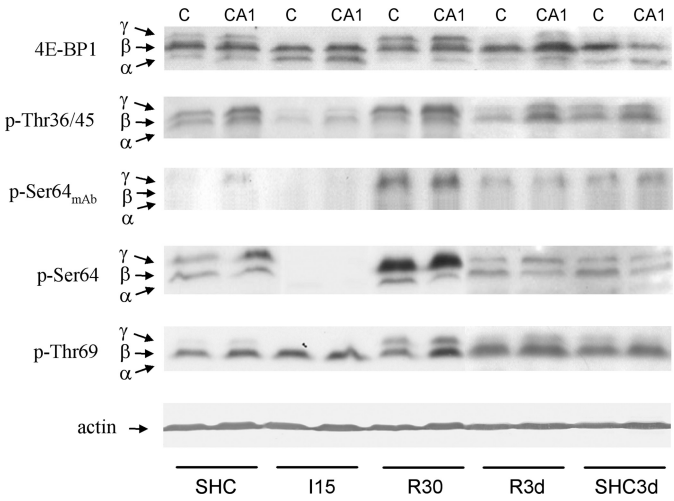

FIGURE 1. **Identification of 4E-BP1 phosphorylation sites induced by ischemia and IR stress.** Samples of cerebral cortex (*C*) or hippocampal CA1 region from control (*SHC* and *SHC3d*) and ischemic animals, without (*I15*) or with reperfusion (*R30* and *R3d*), were subjected to Western blotting for anti-4E-BP1 (*4E-BP1*), anti-phospho-4E-BP1 Thr^{36}/Thr^{45} (*p-Thr36/45*), anti-phospho-4E-BP1 Ser^{64} 174A9 (*p-Ser64$_{mAb}$*), anti-phospho-4E-BP1 Ser^{64} (*p-Ser64*), and anti-phospho-4E-BP1 Thr^{69} (*p-Thr69*) antibodies. *Arrows* show the α, β, and γ forms of 4E-BP1. The phospho-Ser^{64} antibody is also reactive to phospho-Ser^{100} (23). The figures are representative results of 4–6 independent experiments. Quantification of the Western blots is shown in the supplemental material.

To identify the phosphorylation sites implicated in ischemia and IR stress, we used phospho-specific antibodies for the regulated sites of 4E-BP1, Thr^{36}/Thr^{45}, Ser^{64}, and Thr^{69}. Thr^{36}/Thr^{45} phosphorylation was detected in the β and γ forms of 4E-BP1, but not in the α form (Fig. 1, *p-Thr36/45*). I15 induced significant dephosphorylation at Thr^{36}/Thr^{45} in the β and γ forms, whereas R30 induced 4E-BP1 phosphorylation at Thr^{36}/Thr^{45} in the γ form when compared with the controls (Fig. 1, *p-Thr36/45*; supplemental Fig. S2). Ser^{64} phosphorylation, using 174A9 monoclonal antibody, was detected only in the γ form of 4E-BP1 (Fig. 1, *p-Ser64$_{mAb}$*). 4E-BP1 phosphorylated at Ser^{64} was residual in the I15 group, and conversely, increased significantly in the R30 group with respect to the controls (Fig. 1, *p-Ser64$_{mAb}$*; supplemental Fig. S3*A*). Similar results were

found using polyclonal anti-phospho-4E-BP1 Ser^{64} antibody, although this antibody also detected the β form in all samples with the exception of I15 (Fig. 1, *p-Ser64*; supplemental Fig. S3*B*). However, this antibody has been reported to react against phospho-4E-BP1 at the Ser^{100} site as well and has also been described in the β form (23). 4E-BP1 phosphorylated at Thr^{69} was detected in the β and γ forms of 4E-BP1, and no Thr^{69} phosphorylation was found in the α form (Fig. 1, *p-Thr69*). Phospho-Thr^{69} was residual in I15 in the γ form, but it remained in the β form with no significant changes when compared with the controls (supplemental Fig. S4). In contrast, R30 significantly phosphorylated the γ form at Thr^{69} site (Fig. 1, *p-Thr69*; supplemental Fig. S4). Long term reperfusion (R3d) did not induce any significant effect on 4E-BP1 phosphorylation with respect to the SHC3d control (Fig. 1; supplemental Figs. S2–S4). The cerebral cortex and hippocampal CA1 region showed similar changes in 4E-BP1 phosphorylation at the regulated sites studied, and no significant changes were found between them under different experimental conditions (Fig. 1; supplemental Figs. S2–S4).

4E-BP1 Analysis by Two-dimensional Electrophoresis Detects Four 4E-BP1 Phosphorylation States—To characterize further the physiological 4E-BP1-phosphorylation status induced by ischemia and after reperfusion, we analyzed 4E-BP1 in the regulated sites by two-dimensional gel electrophoresis and Western blotting. This study was performed in cortical samples because no significant differences were found between the cerebral cortex and the hippocampal CA1 region (see above). In the first dimension, pH 3–10 strips with a nonlinear gradient were used that increased the resolution in the pH 4–6 region that corresponded to the theoretical pI range of 4E-BP1. Four different spots were detected in the SHC and SHC3d controls (Fig. 2). The first spot was the most basic (pI = 5.85) and corresponded to the hypophosphorylated α form of 4E-BP1; two additional spots, named as β′ and β″, were found and corresponded to the phosphorylated β form; and one additional spot was detected in the most acid position (pI = 4.5) that corresponded to the hyperphosphorylated γ form (Fig. 2, *SHC* and *SHC3d*). I15 induced an increase in the α spot of 4E-BP1 (Fig. 2, *I15*). R30 induced an increase in the β and γ spots when compared with the SHC control (Fig. 2, *R30*). No apparent changes were found among the different spots after long term reperfusion (R3d) with respect to the SHC3d or SHC controls (Fig. 2, *R3d*). These results showed that the β form comprised two different 4E-BP1 phosphorylation states, one basic β′ spot (mainly detected in the I15 group) and another more acid β″ spot (mainly detected in the R30 group), in which phospho-Thr^{36}/Thr^{45} and -Thr^{69} were detected (Figs. 1 and 2). The I15 group had dephosphorylation at Thr^{36}/Thr^{45} and Thr^{36}/Thr^{45}/Ser^{64} residues in the β and γ forms, respectively (Fig. 1), and where β″ and γ spots were undetectable (Fig. 2, *I15*).

4E-BP1 Is Sequentially Phosphorylated at Thr^{69}, Thr^{36}/Thr^{45}, and Ser^{64} Sites—To assess the results described above, we analyzed the phosphorylated residues in 4E-BP1 by two-dimensional gel electrophoresis and Western blotting with the corresponding anti-phospho-4E-BP1 antibodies. Thus, phospho-Thr^{69} was detected in the β′ spot (Fig. 3, *p-Thr69 I15*) and in the β″ and γ spots (Fig. 3, *p-Thr69 R3d*). Phosphorylation at the

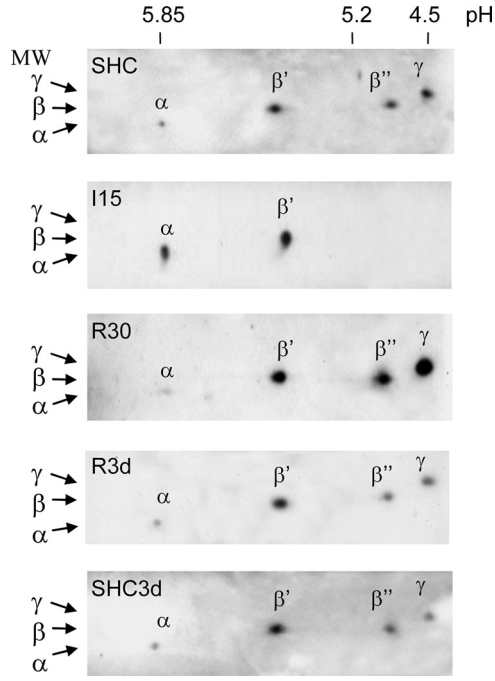

FIGURE 2. **Analysis of 4E-BP1 by two-dimensional gel electrophoresis and changes induced by ischemia and IR stress.** Samples of cerebral cortex from control (*SHC* and *SHC3d*) and ischemic animals, without (*I15*) or with reperfusion (*R30* and *R3d*), were subjected to two-dimensional gel electrophoresis and Western blotting for anti-4E-BP1 antibody. The antibody-reactive spots were named as α, β′, β″, and γ. *Arrows* indicate the relative positions for the α, β, and γ forms of 4E-BP1 in the molecular weight (*MW*) axis. The figures are representative results of 4 independent experiments.

Thr^{36}/Thr^{45} sites was detected in the β″ and γ spots (Fig. 3, *p-Thr36/45 R3d*) but not in the β′ spot (Fig. 3, *p-Thr36/45 R3d* and *p-Thr36/45 I15*). Finally, as expected, phospho-Ser^{64} was only detected in the γ spot (Fig. 3, *p-Ser64$_{mAb}$*). The results were shown with R3d because this condition had a balanced mixture of the four spots (Fig. 2). I15 conditions were shown because it was essential to determine the α and β′ phosphorylation status. These experiments demonstrated that: (i) the α form corresponded to 4E-BP1 dephosphorylated at Thr^{36}/Thr^{45}, Ser^{64}, and Thr^{69} because none of these anti-phospho-4E-BP1 antibodies showed a reaction; (ii) the β form was phosphorylated at Thr^{69}, which was detected at the β′ position, and it was not phosphorylated at Thr^{36}/Thr^{45}; (iii) an additional β form was detected at the β″ position, which had both phospho-Thr^{36}/Thr^{45} and phospho-Thr^{69}; and (iv) the γ form was the hyperphosphorylated 4E-BP1 with specific phospho-Ser^{64} reaction, had phosphorylation at Thr^{36}/Thr^{45} and Thr^{69} sites, and was detected at the more acidic position (Figs. 1–3).

Phosphorylation-dependent Association of 4E-BP1 to eIF4E—The assembly of the eIF4F complex is usually defined operationally as the association of eIF4G to eIF4E. We studied the phosphorylation status of 4E-BP1 associated with eIF4E and the binding of eIF4G to eIF4E as eIF4F complex formation. eIF4E is identified by its ability to bind to the 5′ cap structure and was consequently isolated by affinity chromatography in m^{7}GTP-Sepharose, a cap-containing matrix, and we analyzed the binding partners eIF4G and 4E-BP1 (5, 19). The 4E-BP1 α and β forms were the forms bound to eIF4E, whereas the γ form was absent (Fig. 4, *4E-BP1*). R30 induced a significant decrease

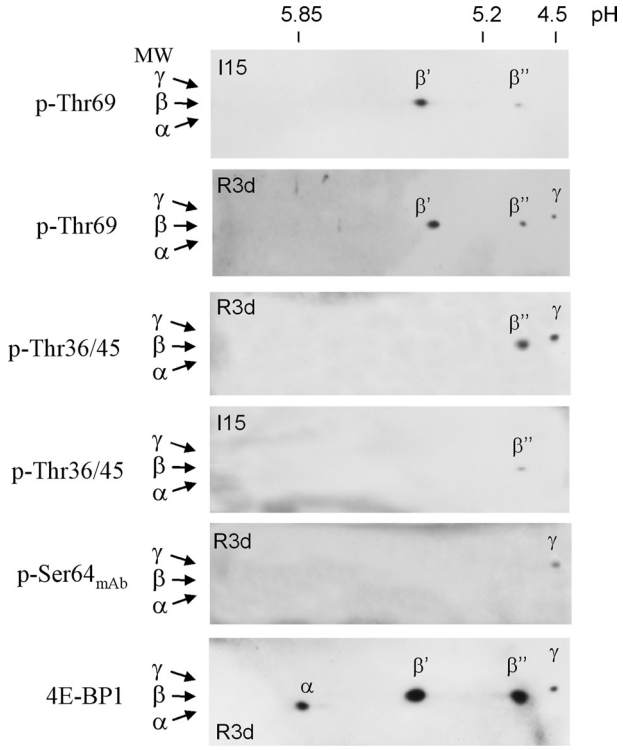

FIGURE 3. **Identification of the phosphorylation regulator sites for 4E-BP1 spots identified by two-dimensional gel electrophoresis.** Samples of cerebral cortex from ischemic animals, without (*I15*) or with long term reperfusion (*R3d*), were subjected to two-dimensional gel electrophoresis and Western blotting for phospho-specific antibodies to 4E-BP1 Thr^{69} (*p-Thr69*), Thr^{36}/Thr^{45} (*p-Thr36/45*), and Ser^{64} 174A9 ($p\text{-}Ser64_{mAb}$). The detected antibody-reactive spots for anti-4E-BP1 antibody (*4E-BP1*) are shown. *Arrows* indicate the relative positions for the α, β, and γ forms of 4E-BP1 in the molecular weight (*MW*) axis. The figures are representative results of 3 independent experiments.

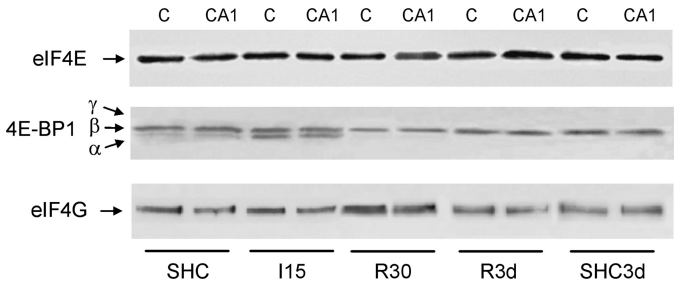

FIGURE 4. **4E-BP1 and eIF4G association with eIF4E.** Samples of cerebral cortex (*C*) or hippocampal CA1 region from control (*SHC* and *SHC3d*) and ischemic animals, without (*I15*) or with reperfusion (*R30* and *R3d*), were bound to m^7GTP-Sepharose and eIF4E, and eIF4E-associated proteins were subjected to SDS-PAGE followed by Western blotting for anti-eIF4E (*eIF4E*), anti-4E-BP1 (*4E-BP1*), and anti-eIF4G (*eIF4G*) antibodies. *Arrows* show the relative positions for eIF4E, eIF4G, and the α, β, and γ forms of 4E-BP1. The figures are representative results of 4–6 independent experiments. Quantification of the 4E-BP1 and eIF4G associated with eIF4E in the different experimental conditions are shown in the supplemental material.

in 4E-BP1 bound to eIF4E when compared with the SHC control or I15 condition, and accordingly, induced a significant increase in eIF4G/eIF4E association (Fig. 4; supplemental Fig. S5). In the I15 group, the α form of 4E-BP1 associated with eIF4E was marked. No significant changes in 4E-BP1 and eIF4G/eIF4E association were found in the R3d group when compared with the SHC3d control or between the cerebral cortex and hippocampal CA1 region (supplemental Fig. S5).

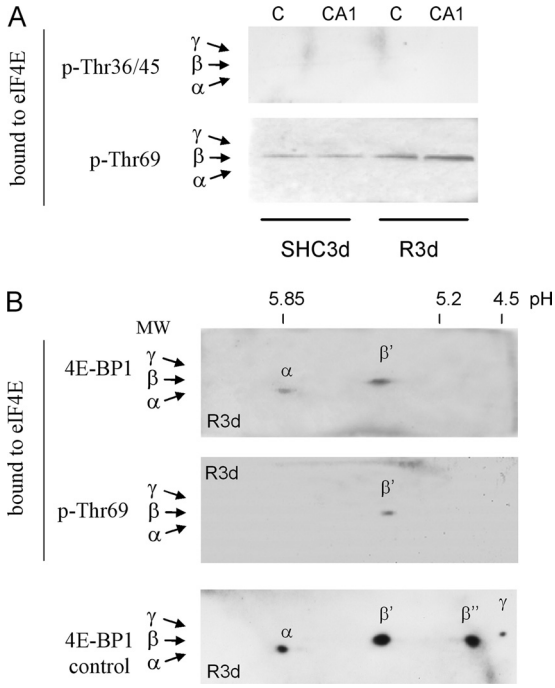

FIGURE 5. **Phosphorylation status of 4E-BP1 associated with eIF4E.** Samples of cerebral cortex (*C*) or hippocampal CA1 region from control (*SHC3d*) and ischemic animals, with long term reperfusion (*R3d*), were bound to m^7GTP-Sepharose and eIF4E-associated 4E-BP1 subjected to SDS-PAGE (*A*) or two-dimensional gel electrophoresis (*B*) and Western blotting for anti-4E-BP1 antibody (*4E-BP1*), or phospho-specific antibodies to 4E-BP1 Thr^{69} (*p-Thr69*), and Thr^{36}/Thr^{45} (*p-Thr36/45*). *Arrows* show the relative positions for the α, β, and γ forms of 4E-BP1. Spots detected with anti-4E-BP1 antibody from Fig. 3 are shown as control (*4E-BP1 control*). The figures are representative results of 3 independent experiments.

We studied the phosphorylation of Thr^{36}/Thr^{45}, Ser^{64}, and Thr^{69} in the 4E-BP1 that was bound to eIF4E. Phospho-Thr^{69} was detected in the β form, whereas phospho-Thr^{36}/Thr^{45} was not (Fig. 5*A*), and neither was phospho-Ser^{64} in accordance with the absence of the γ form (data not shown). These results were observed in the cerebral cortex and hippocampal CA1 region. Two-dimensional gel electrophoresis and Western blotting of 4E-BP1 bound to eIF4E detected the α and β′ spots of 4E-BP1, whereas the β″ and γ spots were not present (Fig. 5*B*, *4E-BP1*). Accordingly, the β′ spot corresponded to phosphorylation of 4E-BP1 at Thr^{69} (Fig. 5*B*, *p-Thr69*), and phospho-Thr^{36}/Thr^{45} and phospho-Ser^{64} were not detected (data not shown). R3d was shown in the figure because as described above, it had a balanced mixture of the four spots. These results demonstrated that the hypophosphorylated α form and Thr^{69}-phosphorylated β form of 4E-BP1 were specific forms bound to eIF4E. No 4E-BP1 phosphorylated at $Thr^{69}/Thr^{36}/Thr^{45}$ nor $Thr^{69}/Thr^{36}/Thr^{45}$/Ser64 was associated with eIF4E.

Ischemic Stress Induces mTOR and Akt Dephosphorylation at Ser^{2448} and Ser^{473}, and IR Stress Restores or Induces Phosphorylation—Finally, we studied the phosphorylation of mTOR at Ser^{2448}, a residue that is correlated with kinase activity (24), and the activity of the upstream effector of mTORC1, the serine/threonine-protein kinase Akt (also named protein kinase B), through phosphorylation at Thr^{308} and Ser^{473} (25). I15 induced a significant decrease in mTOR phosphorylation at the Ser^{2448} site, which was restored to control levels upon

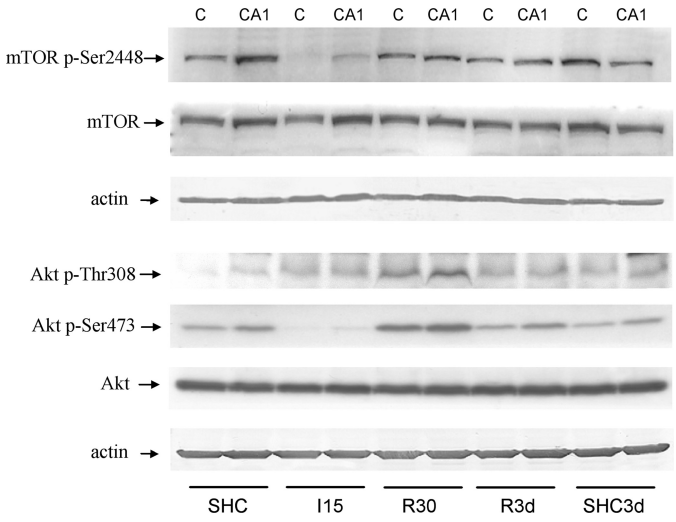

FIGURE 6. **Changes in mTOR and Akt phosphorylation induced in ischemia and IR stress.** Samples of cerebral cortex (*C*) or hippocampal CA1 region from control (*SHC* and *SHC3d*) and ischemic animals, without (*I15*) or with reperfusion (*R30* and *R3d*), were subjected to Western blotting for anti-mTOR (*mTOR*) and anti-phospho-mTOR Ser^{2448} (*mTOR p-Ser2448*), or anti-Akt (*Akt*), anti-phospho-Akt Thr^{308} (*Akt p-Thr308*), and anti-phospho-Akt Ser^{473} (*Akt p-Ser473*) antibodies. *Arrows* show the relative positions for mTOR or Akt. The figures are representative results of 4 independent experiments. Quantification of the Western blots is shown in the supplemental material.

reperfusion (R30 or R3d), with the exception of CA1 SHC that had increased Ser^{2448} phosphorylation (Fig. 6; supplemental Fig. S6). In addition, I15 induced a significant decrease in Akt phosphorylation at the Ser^{473} site, whereas R30 significantly induced Thr^{308} and Ser^{473} phosphorylation when compared with the controls (Fig. 6; supplemental Fig. S7). No significant changes were found in mTOR and Akt phosphorylation in the R3d group with respect to the SHC3d control.

DISCUSSION

Phosphorylation of 4E-BP1 at several sites stimulated by insulin and other agents is described as hierarchical, with phosphorylation of Thr^{36}/Thr^{45} being required for modification of Thr^{69}, which precedes phosphorylation of Ser^{64} and release from eIF4E (6, 10). The other three identified phosphorylation sites, Ser^{82}, Ser^{100}, and Ser^{111}, are constitutive or without regulatory function on 4E-BP1 (6, 7). It is important to highlight that all these findings have been studied in stimulated cultured cells, including cell lines and transfected cells. Therefore, physiological studies that demonstrate the control of 4E-BP1 remain to be completed. Phosphorylation-dependent 4E-BP1 activity is controlled by mTORC1, which is known to operate as an oxygen and energy sensor for the cells, because hypoxia and energy deprivation induce mTORC1 inhibition (11). Ischemia induces a period of hypoxia that induces energy depletion that is restored in the following reperfusion period upon reoxygenation (12). The present study was a physiological investigation of 4E-BP1 regulation by phosphorylation, using control conditions and ischemic and IR stress in brain tissue, and described a new hierarchical phosphorylation of 4E-BP1. We revealed 4E-BP1 in four phosphorylation states: dephosphorylated; phosphorylated at the Thr^{69} site; Thr^{69}- and Th^{36}/Thr^{45}-phosphorylated; and Thr^{69}/Th^{36}/Thr^{45}-phosphorylated in addition to Ser^{64} phosphorylation. These corresponded in two-dimensional gel electrophoresis to the α, β', β'', and γ spots, respectively. 4E-BP1 phosphorylated at Thr^{69} was detected alone in the more basic β form, β'. Phospho-Thr^{69} was also identified in the β'' and γ form, together with phospho-Thr^{36}/Thr^{45} and -Thr^{36}/Thr^{45}/Ser^{64}, respectively. 4E-BP1 phosphorylated at Thr^{36}/Thr^{45} was identified in the β'' (more acid than β') and γ form, which also had phospho-Thr^{69} and phospho-Thr^{69}/Ser^{64}, respectively. In addition, Ser^{64} phosphorylation was detected together with Thr^{69}/Th^{36}/Thr^{45} phosphorylation and was specific and differentiated to the γ form as the more acid state of 4E-BP1. Dephosphorylated 4E-BP1 may be constitutively phosphorylated at other sites described for 4E-BP1 (6, 7), with the exception of Ser^{100} that was not detected in the α form.

Ischemic stress induced 4E-BP1 dephosphorylation at Thr^{69}, Thr^{36}/Thr^{45}, and Ser^{64} residues, with 4E-BP1 remaining phosphorylated at Thr^{69} alone or dephosphorylated. In the subsequent reperfusion period, 4E-BP1 phosphorylation was induced at Thr^{36}/Thr^{45} and Ser^{64}, in addition to Thr^{69}. After long term reperfusion and in controls, the levels of 4E-BP1 phosphorylated in Thr^{69} or Thr^{69}/Th^{36}/Thr^{45} were higher than in Thr^{69}/Th^{36}/Thr^{45}/Ser^{64}.

All β and γ forms of 4E-BP1 had phospho-Thr^{69}, and the reaction against anti-phospho-4E-BP1 Thr^{69} antibody was correlated with the anti-4E-BP1 antibody reaction in the β and γ forms ($r = 0.9666$, $p < 0.0001$, by Pearson correlation test for γ/β ratio). Therefore, there was phosphorylation of Thr^{69} without phospho-Th^{36}/Thr^{45}/Ser^{64} (β' form), and no Thr^{36}/Thr^{45} phosphorylation alone was detected or without Thr^{69} phosphorylation under all experimental conditions, including the controls. In addition, under ischemic stress, 4E-BP1 was phosphorylated at Thr^{69} alone. We concluded from these results that Thr^{69} phosphorylation was the first event. Besides, because there was phosphorylation of Thr^{36}/Thr^{45} without phospho-Ser^{64} (β'' form), Ser^{64} phosphorylation was not detected without both Thr^{69} and Th^{36}/Thr^{45} phosphorylation under any control or stress conditions, and neither was phosphorylation of Ser^{64} alone detected. And, in addition, during the long term reperfusion and control condition, the level of Th^{36}/Thr^{45} phosphorylation was higher than the phospho-Th^{36}/Thr^{45}/Ser^{64}. These results demonstrated that phosphorylation of Th^{36}/Thr^{45} proceeds to Ser^{64}. Finally, if phosphorylation of 4E-BP1 at Th^{36}/Thr^{45} alone without phospho-Thr^{69} is present, a new spot might be detected in two-dimensional experiments. In a similar fashion, Ser^{64} phosphorylation alone might also be detected in two dimensions as a new spot or in combination with phospho-Thr^{69}. However, just four spots were detected for 4E-BP1 under control, ischemic, or reperfusion conditions that corresponded to unphosphorylated, Thr^{69} phosphorylated, phospho-Thr^{69} plus Th^{36}/Thr^{45} phosphorylation, and all phosphorylations together with phospho-Ser^{64}.

These results conclude a new hierarchical phosphorylation for 4E-BP1 in which Thr^{69} phosphorylation is the priming event for subsequent phosphorylation of Thr^{36}/Thr^{45}, which precedes phosphorylation of Ser^{64}. This alternative model to the established hierarchy (10) (Table 1) is in accordance with some reports that have described phosphorylation of Thr^{69} independently of Thr^{36}/Thr^{45} phosphorylation in cultured cells (9, 26–29). Our results confirm the compelling evidence of a

TABLE 1
Characteristics of 4E-BP1 phosphorylated at regulated sites in the established model and new model described in this study

Phosphorylation hierarchy	Phosphorylation status in the form*: α	β	γ	Binding to eIF4E	Not binding to eIF4E	Ref.
un-P[1] → Thr^{36}/Thr^{45} → Thr^{69} → Ser^{64}	Thr^{36}/Thr^{45} un-P	Thr^{36}/Thr^{45}/Thr^{69} [2]	Thr^{36}/Thr^{45}/Thr^{69}/Ser^{64}	un-P Thr^{36}/Thr^{45} [3]	Thr^{36}/Thr^{45}/Thr^{69}/Ser^{64} [4]	(6,9,10,36)
un-P → Thr^{69} → Thr^{36}/Thr^{45} → Ser^{64}	un-P	Thr^{69} Thr^{69}/Thr^{36}/Thr^{45}	Thr^{69}/Thr^{36}/Thr^{45}/Ser^{64}	un-P Thr^{69}	Thr^{69}/Thr^{36}/Thr^{45} Thr^{69}/Thr^{36}/Thr^{45}/Ser^{64}	this paper

* 4E-BP1 forms resolved in SDS-PAGE in order of decreasing electrophoretic mobility.
[1] Un-P, un-phosphorylated 4E-BP1 at regulated sites: Thr^{36}, Thr^{45}, Ser^{64}, and Thr^{69} (+1 in the human sequence).
[2] Thr^{69} phosphorylation independently of Thr^{36}/Thr^{45} has been reported (9,26–29).
[3] 4E-BP1 peptides phosphorylated on Ser^{64} or Ser^{64}/Thr^{69} alone allow binding to eIF4E (10).
[4] Ser^{64} phosphorylation may be dispensable for dissociation from eIF4E (29).

triphosphorylated 4E-BP1 status that is required for phosphorylation at Ser^{64} (6, 7). In addition, the results showed that Thr^{36}/Thr^{45} phosphorylation was detected in the β and γ forms and that Ser^{64} phosphorylation was detected in the γ form, as described by others (9, 29, 30). Besides, Thr^{36}/Thr^{45} phosphorylation did not induce any shift in the apparent molecular weight of 4E-BP1, and it was phospho-Thr^{69} that induced the shift to the β form, whereas phospho-Ser^{64} induced the shift to the γ form, in accordance with other studies (29, 30). Table 1 summarizes the hierarchical phosphorylation pathway and characteristics of phosphorylated 4E-BP1 in the established model and new model described here.

This study was performed in brain, where 4E-BP2 is largely expressed (31). However, 4E-BP1 has been described as a specific target in several specific brain diseases, such as cerebral alcohol toxicity, Alzheimer disease, glioma (32–34), and cerebral ischemia (16, 35), which indicates a particular role for 4E-BP1 in brain. In addition, results of 4E-BP2 phosphorylation from our laboratory showed that in contrast to 4E-BP1, IR stress did not induce any change in 4E-BP2 isoforms, their levels were not modified by phosphorylation at studied Thr^{36}/Thr^{45} sites, and this phosphorylation did not alter the proportion between the isoforms.[4] In conclusion, the response to IR stress was weaker for 4E-BP2 when compared with 4E-BP1 as the change in phosphorylation of 4E-BP2 was less pronounced.

This study also addressed the role of 4E-BP1 phosphorylation in the activity of eIF4E. The individual contribution of the 4E-BP1 phosphorylation sites to the control of eIF4E binding remains controversial. 4E-BP1 phosphorylated on Th^{36}/Thr^{45} retains the ability to interact with eIF4E (10). Phosphorylation at Ser^{64} and Thr^{69} seems to regulate binding to eIF4E, but these phosphorylation reactions alone are insufficient to block binding to eIF4E, which indicates that combination with Thr^{36}/Thr^{45} phosphorylation is necessary to dissociate 4E-BP1 from eIF4E (6, 10, 36). However, Ser^{64} phosphorylation might be dispensable for dissociation from eIF4E (29), and it has suggested that phosphorylation at this site prevents the reassociation of eIF4E and 4E-BP1 (37). In contrast, other studies have shown that Thr^{69} phosphorylation is crucial for dissociation from eIF4E (23, 37, 38). Our results demonstrate that Thr^{69} phosphorylation alone allows binding to eIF4E, and subsequent Thr^{36}/Thr^{45} phosphorylation is sufficient to dissociate 4E-BP1 from eIF4E. The R3d group had a significant amount of 4E-BP1 phosphorylated at Thr^{69}/Thr^{36}/Thr^{45}, and neither was associated with eIF4E; therefore, we share the hypothesis that Ser^{64} phosphorylation is dispensable for dissociation from eIF4E. IR stress during short term reperfusion induced a significant decrease in 4E-BP1/eIF4E association, parallel to the increased eIF4G/eIF4E association and in accordance with the induced 4E-BP1 phosphorylation at Thr^{36}/Thr^{45} and Ser^{64}, in addition to Thr^{69}. Table 1 shows the phosphorylation-dependent 4E-BP1 interaction with eIF4E according to the conventional and the new model. In the model described here, signaling pathways leading to Thr^{36}/Thr^{45} phosphorylation would induce the release of 4E-BP1 from eIF4E and eIF4E activation. On the contrary, in the established model, these signaling pathways would retain 4E-BP1 associated with eIF4E, thus inhibiting eIF4E. Moreover, in this new model, in the event of the phosphorylation on Thr^{69}, 4E-BP1 would remain associated with eIF4E, whereas in the conventional model, this might not occur. This different response could have physiological consequences.

The new sequence in the phosphorylation of 4E-BP1 suggests that it may be brain tissue-specific. We have done experiments with primary neuronal cells in culture subjected to oxygen-glucose deprivation, an *in vitro* ischemia model (39), and compared them with neuronal cells under insulin deprivation (40). Insulin treatment of cells after deprivation is known to modify phosphorylation of 4E-BP1 at Thr^{36}/Thr^{45} as the first event in cell lines (9, 23, 29, 37). Oxygen-glucose deprivation or insulin deprivation induced dephosphorylation of 4E-BP1 at Thr^{36}/Thr^{45} and Ser^{64} residues in the γ form, with 4E-BP1 remaining phosphorylated at Thr^{69} and dephosphorylated at Thr^{36}/Thr^{45} in the β form in neuronal cells. The subsequent reperfusion or insulin treatment induced 4E-BP1 phosphorylation at Thr^{36}/Thr^{45} and Ser^{64}, in addition to Thr^{69} (supplemental Fig. S8). In addition, all the β form of 4E-BP1 was phosphorylated at Thr^{69} (phospho-Thr^{69} reaction correlated with 4E-BP1 levels; $r = 0.988$, $p < 0.0016$, by Pearson correlation test), whereas Thr^{36}/Thr^{45} phosphorylation was only detected in a fraction of the β form. These results indicated that 4E-BP1 was phosphorylated at Thr^{36}/Thr^{45} secondly in neuronal cells, in a similar fashion to the results described here, which suggests

[4] M. I. Ayuso and A. Alcázar, unpublished results.

that the brain tissues show a new hierarchical phosphorylation for 4E-BP1 in response to stress.

4E-BP1 is a direct target of mTORC1, which is known to control 4E-BP1 activity. Activation of mTORC1 leads to hyperphosphorylation of 4E-BP1, and therefore, the phosphorylation status of 4E-BP1 is an indicator of mTORC1 activity (6, 7, 38). In addition, activation of mTORC1 is correlated with the phosphorylation of mTOR at Ser^{2448} in a PI3-kinase/Akt signaling-dependent fashion (24). Our results showed that inhibition of mTORC1 activity was induced by ischemic stress, which was confirmed by a significant decrease in 4E-BP1 and mTOR-Ser^{2448} phosphorylation. This agrees with the known decrease in mTORC1 activity that is induced by energy depletion and hypoxic conditions (11). In addition, mTOR autophosphorylation at Ser^{2481} (24) was also decreased by ischemia (data not shown). The mTOR phosphorylation at Ser^{2448} (and Ser^{2481} autophosphorylation) and 4E-BP1 phosphorylation were restored during reperfusion and returned to control values. However, during short term but not long term reperfusion, phosphorylation of 4E-BP1 was increased above the control level, with a significant increase in the hyperphosphorylated γ form, whereas mTOR phosphorylation remained at control levels. It is known that the initial period of reperfusion the reoxygenation increases ROS production (13). Also, it has been reported that ROS inhibit protein phosphatase 2A (PP2A) (41, 42), phosphatase activity that has been implicated in regulation of 4E-BP1 phosphorylation (7, 30, 43). 4E-BP1 phosphorylation at Ser^{64}, but not Thr^{69}, is induced by ROS (44). We hypothesized that inhibition of PP2A-type activity induced by ROS produced during short term reperfusion could explain the increase in hyperphosphorylated 4E-BP1 at this time. Additionally, the reported inhibition of PP2A activity by mTORC1 (43, 45, 46) could not be excluded.

mTOR is a downstream kinase in the PI3-kinase/Akt signaling pathway. Activation of Akt involves two sequential phosphorylations at Thr^{308} (essential for Akt activity) and Ser^{473} (necessary for its highest activity *in vitro*) (25). We found a significant decrease in Ser^{473} phosphorylation in ischemic stress that was related to the decreased mTOR phosphorylation at Ser^{2448}. On the other hand, the increase in Thr^{308} and Ser^{473} phosphorylation in short term reperfusion could be explained by the inhibition of PP2A by ROS because PP2A has been described as an Akt phosphatase (47).

Recent studies have indentified a second regulatory motif in 4E-BP1, named RAIP (according to its sequence) (7, 9, 23). RAIP motif has a direct effect on mTOR-dependent phosphorylation of Thr^{36}/Thr^{45} sites, whereas TOS motif primarily affects phosphorylation of Thr^{69} and also Ser^{64} (9, 23). TOS motif is required for interaction with raptor, a mTOR modulator in mTORC1. However, RAIP motif seems to be independent of the 4E-BP1/raptor interaction and may interact with another putative partner protein (7, 9, 23). Therefore, there are two mTOR-dependent inputs that regulate the phosphorylation sites in 4E-BP1. Depending on the cell type, one of them could be activated by a basal stimulus, inducing the phosphorylation on Thr^{36}/Thr^{45} or Thr^{69} (as the first event) and resulting in the established or new phosphorylation hierarchy, respectively. We hypothesize that in brain tissue, the mTORC1 signal could be primarily operating through TOS motif, inducing 4E-BP1 phosphorylation at Thr^{69}.

4E-BP1 is one of the two best characterized targets of mTORC1, which is crucial in cancer control (48). 4E-BP1 has a key role in cancer because its inactivation by phosphorylation leads to increased eIF4F complex formation, and consequently, enhanced cap-dependent translation and cell growth. Thus, its deregulation has been implicated in several types of cancer (49) including nervous tissue tumor cells (34). However, no data are available about the phosphorylation sites for 4E-BP1 regulation under physiological conditions, and information about this might be important for cancer control. This study showed a new sequence in the phosphorylation of 4E-BP1 and demonstrated advances to elucidate its physiological role, which could be of great interest in cancer control.

Acknowledgment—We are indebted to M. Gómez-Calcerrada for technical assistance.

REFERENCES

1. Clemens, M. J., and Bommer, U. A. (1999) *Int. J. Biochem. Cell Biol.* **31,** 1–23
2. Hershey, J. W. B., and Merrick, W. C. (2000) in *Translational Control of Gene Expression* (Sonenberg, N., Hershey, J. W. B., and Mathews, M. B., eds) pp. 33–88, Cold Spring Harbor Laboratory Press, New York
3. Pestova, T., Lorsch, J. R., and Hellen, C. U. T. (2007) in *Translational Control in Biology and Medicine* (Mathews, M. B., Sonenberg, N., and Hershey, J. W. B., eds) pp. 87–128, Cold Spring Harbor Laboratory Press, New York
4. Rhoads, R. E. (2009) *J. Biol. Chem.* **284,** 16711–16715
5. Gingras, A. C., Gygi, S. P., Raught, B., Polakiewicz, R. D., Abraham, R. T., Hoekstra, M. F., Aebersold, R., and Sonenberg, N. (1999) *Gene. Dev.* **13,** 1422–1437
6. Proud, C. G. (2007) *Biochem. J.* **403,** 217–234
7. Raught, B., and Gingras, A. C. (2007) in *Translational Control in Biology and Medicine* (Mathews, M. B., Sonenberg, N., and Hershey, J. W. B., eds) pp. 369–400, Cold Spring Harbor Laboratory Press, New York
8. Sonenberg, N., and Hinnebusch, A. G. (2009) *Cell* **136,** 731–745
9. Wang, X., Beugnet, A., Murakami, M., Yamanaka, S., and Proud, C. G. (2005) *Mol. Cell. Biol.* **25,** 2558–2572
10. Gingras, A. C., Raught, B., Gygi, S. P., Niedzwiecka, A., Miron, M., Burley, S. K., Polakiewicz, R. D., Wyslouch-Cieszynska, A., Aebersold, R., and Sonenberg, N. (2001) *Gene. Dev.* **15,** 2852–2864
11. Ma, X. M., and Blenis, J. (2009) *Nat. Rev. Mol. Cell Biol.* **10,** 307–318
12. White, B. C., Sullivan, J. M., DeGracia, D. J., O'Neil, B. J., Neumar, R. W., Grossman, L. I., Rafols, J. A., and Krause, G. S. (2000) *J. Neurol. Sci.* **179,** 1–33
13. Warner, D. S., Sheng, H., and Batinić-Haberle, I. (2004) *J. Exp. Biol.* **207,** 3221–3231
14. Lipton, P. (1999) *Physiol. Rev.* **79,** 1431–1568
15. Kirino, T. (2000) *Neuropathology* **20,** S95-S97
16. Martín de la Vega, C., Burda, J., Nemethova, M., Quevedo, C., Alcázar, A., Martín, M. E., Danielisova, V., Fando, J. L., and Salinas, M. (2001) *Biochem. J.* **357,** 819–826
17. Burda, J., Martín, M. E., García, A., Alcázar, A., Fando, J. L., and Salinas, M. (1994) *Biochem. J.* **302,** 335–338
18. García-Bonilla, L., Cid, C., Alcázar, A., Burda, J., Ayuso, I., and Salinas, M. (2007) *J. Neurochem.* **103,** 1368–1380
19. Quevedo, C., Salinas, M., and Alcázar, A. (2002) *Biochem. Biophys. Res. Commun.* **291,** 560–566
20. Cid, C., Alvarez-Cermeño, J. C., Camafeita, E., Salinas, M., and Alcázar, A. (2004) *FASEB J.* **18,** 409–411
21. Cid, C., Garcia-Bonilla, L., Camafeita, E., Burda, J., Salinas, M., and Alcazar, A. (2007) *Proteomics* **7,** 3207–3218

22. Proud, C. G., and Denton, R. M. (1997) *Biochem. J.* **328,** 329–341
23. Beugnet, A., Wang, X., and Proud, C. G. (2003) *J. Biol. Chem.* **278,** 40717–40722
24. Copp, J., Manning, G., and Hunter, T. (2009) *Cancer Res.* **69,** 1821–1827
25. Manning, B. D., and Cantley, L. C. (2007) *Cell* **129,** 1261–1274
26. Heesom, K. J., and Denton, R. M. (1999) *FEBS Lett.* **457,** 489–493
27. Mothe-Satney, I., Yang, D., Fadden, P., Haystead, T. A., and Lawrence, J. C., Jr. (2000) *Mol. Cell. Biol.* **20,** 3558–3567
28. Mothe-Satney, I., Brunn, G. J., McMahon, L. P., Capaldo, C. T., Abraham, R. T., and Lawrence, J. C., Jr. (2000) *J. Biol. Chem.* **275,** 33836–33843
29. Ferguson, G., Mothe-Satney, I., and Lawrence, J. C., Jr. (2003) *J. Biol. Chem.* **278,** 47459–47465
30. Guan, L., Song, K., Pysz, M. A., Curry, K. J., Hizli, A. A., Danielpour, D., Black, A. R., and Black, J. D. (2007) *J. Biol. Chem.* **282,** 14213–14225
31. Tsukiyama-Kohara, K., Vidal, S. M., Gingras, A. C., Glover, T. W., Hanash, S. M., Heng, H., and Sonenberg, N. (1996) *Genomics* **38,** 353–363
32. Li, Q., and Ren, J. (2007) *Exp. Neurol.* **204,** 840–844
33. Damjanac, M., Rioux Bilan, A., Paccalin, M., Pontcharraud, R., Fauconneau, B., Hugon, J., and Page, G. (2008) *Neurobiol. Dis.* **29,** 354–367
34. Ermoian, R. P., Kaprealian, T., Lamborn, K. R., Yang, X., Jelluma, N., Arvold, N. D., Zeidman, R., Berger, M. S., Stokoe, D., and Haas-Kogan, D. A. (2009) *J. Neurooncol.* **91,** 19–26
35. Lu, A., Tang, Y., Ran, R., Clark, J. F., Aronow, B. J., and Sharp, F. R. (2003) *J. Cereb. Blood Flow Metab.* **23,** 786–810
36. Niedzwiecka, A., Marcotrigiano, J., Stepinski, J., Jankowska-Anyszka, M., Wyslouch-Cieszynska, A., Dadlez, M., Gingras, A. C., Mak, P., Darzynkiewicz, E., Sonenberg, N., Burley, S. K., and Stolarski, R. (2002) *J. Mol. Biol.* **319,** 615–635
37. Wang, X., Li, W., Parra, J. L., Beugnet, A., and Proud, C. G. (2003) *Mol. Cell. Biol.* **23,** 1546–1557
38. Proud, C. G. (2004) *Biochem. Biophys. Res. Commun.* **313,** 429–436
39. Martín, M. E., Muñoz, F. M., Salinas, M., and Fando, J. L. (2000) *Biochem. J.* **351,** 327–334
40. Quevedo, C., Alcázar, A., and Salinas, M. (2000) *J. Biol. Chem.* **275,** 19192–19197
41. Raghuraman, G., Rai, V., Peng, Y. J., Prabhakar, N. R., and Kumar, G. K. (2009) *Antioxid. Redox Signal* **11,** 1777–1789
42. Clerkin, J. S., Naughton, R., Quiney, C., and Cotter, T. G. (2008) *Cancer Lett.* **266,** 30–36
43. Shah, O. J., Anthony, J. C., Kimball, S. R., and Jefferson, L. S. (2000) *Am. J. Physiol. Endocrinol. Metab.* **279,** E715–E729
44. Rocic, P., Seshiah, P., and Griendling, K. K. (2003) *J. Biol. Chem.* **278,** 36973–36979
45. Peterson, R. T., Desai, B. N., Hardwick, J. S., and Schreiber, S. L. (1999) *Proc. Natl. Acad. Sci. U.S.A.* **96,** 4438–4442
46. Harwood, F. C., Shu, L., and Houghton, P. J. (2008) *J. Biol. Chem.* **283,** 2575–2585
47. Trotman, L. C., Alimonti, A., Scaglioni, P. P., Koutcher, J. A., Cordon-Cardo, C., and Pandolfi, P. P. (2006) *Nature* **441,** 523–527
48. Petroulakis, E., Mamane, Y., Le Bacquer, O., Shahbazian, D., and Sonenberg, N. (2006) *Br. J. Cancer* **94,** 195–199
49. Armengol, G., Rojo, F., Castellví, J., Iglesias, C., Cuatrecasas, M., Pons, B., Baselga, J., and Ramón y Cajal, S. (2007) *Cancer Res.* **67,** 7551–7555